J Membrane Biol (2008) 222:31–41
DOI 10.1007/s00232-008-9101-0

Electrophysiological and Fluorescence Microscopy Studies with HERG Channel/EGFP Fusion Proteins

Sonja Claassen · Sarah Schwarzer · Jost Ludwig · Bernd J. Zünkler

Received: 4 January 2008 / Accepted: 13 March 2008 / Published online: 15 April 2008

Abstract HERG (human ether-a-go-go-related gene) encodes the Kv11.1 protein α-subunit that underlies the rapidly activating delayed rectifier K^+ current (I_{Kr}) in the heart. Alterations in the functional properties or membrane incorporation of HERG channels, either by genetic mutations or by administration of drugs, play major roles in the development of life-threatening torsades de pointes cardiac arrhythmias. Visualization of ion channel localization is facilitated by enhanced green fluorescent protein (EGFP) tagging, but this process can alter their properties. The aim of the present study was to characterize the electrophysiological properties and the cellular localization of HERG channels in which EGFP was tagged either to the C terminus (HERG/EGFP) or to the N terminus (EGFP/HERG). These fusion constructs were transiently expressed in human embryonic kidney (HEK) 293 cells, and the whole-cell patch-clamp configuration and a confocal laser scanning microscope with primary anti-HERG antibodies and fluorescently labeled secondary antibodies were used. For EGFP/HERG channels the deactivation kinetics were faster and the peak tail current density was reduced when compared to both wild-type HERG channels and HERG/EGFP channels. Laser scanning microscopic studies showed that both fusion proteins were localized in the cytoplasm and on discrete microdomains in the plasma membrane. The extent of labeling with anti-HERG antibodies of HEK 293 cells expressing EGFP/HERG channels was less when compared to HERG/EGFP channels. In conclusion, both electrophysiological and immunocytochemical studies showed that EGFP/HERG channels themselves have a protein trafficking defect. HERG/EGFP channels have similar properties as untagged HERG channels and, thus, might be especially useful for fluorescence microscopy studies.

Keywords HERG channel · Enhanced green fluorescent protein · Laser scanning confocal microscopy · Patch clamp · Long QT syndrome · Domperidone

S. Claassen · B. J. Zünkler (✉)
Federal Institute for Drugs and Medical Devices,
Kurt-Georg-Kiesinger-Allee 3, 53175 Bonn, Germany
e-mail: j.zuenkler@bfarm.de

S. Schwarzer · J. Ludwig
Molecular Bioenergetics, Institute of Cellular and Molecular Botany, University of Bonn, Kirschallee 1, 53115 Bonn, Germany

Introduction

The congenital long QT syndrome (LQTS) is characterized by delayed cardiac repolarization and a prolonged QT interval in the electrocardiogram. This leads to an increased susceptibility of the heart to the development of life-threatening ventricular arrhythmias (torsades de pointes) (review in Zünkler 2006). HERG (human ether-a-go-go-related gene) encodes the Kv11.1 protein α-subunit that underlies the rapidly activating delayed rectifier K^+ current (I_{Kr}) in the heart, and mutations in HERG result in the proarrhythmic type 2 LQTS (LQT2) (Curran et al. 1995). The HERG channel is composed of four identical α-subunits, and each subunit consists of six transmembrane domains as well as NH_2- and COOH-terminal cytoplasmic tails (Warmke and Ganetzky 1994; Sanguinetti et al. 1995; Trudeau et al. 1995). Forty-five percent of LQTS sufferers harbor HERG mutations, and HERG mutations are most prevalent within the intracellular domains, in the N-terminal region (notably in the PAS domain, which is characteristic for the eag family of K^+ channels) and in the

putative cyclic nucleotide binding domain, but mutation "hot spots" are also observed in the pore region (Splawski et al. 2000). About 200 LQT2-associated HERG mutations have been described. Several mechanisms have been identified, including disruption of Kv11.1 channel synthesis, defective protein trafficking and altered gating or permeation. Most mutations in HERG produce abnormalities in the intracellular transport to the cell surface membrane (protein trafficking) of Kv11.1 channels (Anderson et al. 2006). Protein trafficking defects are often studied using enhanced green fluorescent protein (EGFP) tagged either to the C terminus (HERG/EGFP) or to the N terminus (EGFP/HERG) of HERG channels (for studies employing EGFP/HERG channels, see Teng et al. 2004; Sasano et al. 2004; Paulussen et al. 2002 2005; Furutani et al. 1999; for studies employing HERG/EGFP channels, see Petrecca et al. 1999; Rossenbacker et al. 2005). Several drugs prolong the QT interval, not via direct HERG channel block but indirectly via disruption of HERG channel protein processing and maturation leading to a reduction of its surface plasma membrane expression (arsenic trioxide [Ficker et al. 2004], pentamidine [Kuryshev et al. 2005; Cordes et al. 2005], celastrol [Sun et al. 2006], cardiac glycosides [Wang et al. 2007]). Whereas GFP tagging does not seem to alter the function of some receptors, it is known that GFP alters the function, membrane localization or rate of membrane incorporation of other receptors; e.g., recently Limon et al. (2007) studied the properties of glutamate receptor 3 tagged with GFP at the amino or carboxyl terminus and found that, depending on the site of GFP insertion, the tagging can produce substantial changes in the properties of the receptor. Therefore, the aim of the present study was to characterize the electrophysiological and pharmacological properties and the cellular localization of HERG channels tagged with EGFP either to the C-terminal domain (HERG/EGFP) or to the N-terminal domain (EGFP/HERG) which had been transiently expressed in human embryonic kidney (HEK) 293 cells. The whole-cell configuration of the patch-clamp technique was used to study K^+ currents through the fusion proteins, and immunocytochemical experiments were performed, employing a confocal laser scanning microscope, primary anti-HERG antibodies and fluorescein isothiocyanate (FITC)– or tetramethylrhodamine-isothiocyanate (TRITC)–conjugated secondary antibodies.

Materials and Methods

Plasmid Construction

A HERG (KCNH2, Kv11.1, GenBank accession U04270) expression plasmid (pcDNA3-HERG, designated HERG in the following) was generously provided by Dr. G. Robertson (University of Wisconsin, Madison, WI). The HERG/EGFP expression plasmid containing the coding sequence of EGFP tagged to the C terminus of the HERG channel was generated by fusion of EGFP to the 3′-end of the HERG coding sequence without a linker using a polymerase chain reaction–based overlap extension method (Ho et al. 1989). The EGFP/HERG construct was generated by ligating the HERG coding sequence with a Ser-Gly-Leu-Arg-Ser-Thr-linker to vector pEGFP-C1. Please note that in all three vectors used (pcDNA3, pBK-CMV and pEGFP-C1) the expression of inserted genes is driven by the immediate early cytomegalovirus (CMV) promoter. The pEGFP-C1 vector is identical to pBK-CMV except for the EGFP coding sequence present downstream from the CMV promoter.

Culture and Transfection of HEK 293 Cells

Human embryonic kidney (HEK) 293 cells were plated at a density of 11×10^5/dish (35 mm diameter) and cultured (at 10% CO_2) in Dulbeccós modified Eagle medium (DMEM) with 1 g/l glucose supplemented with 10% fetal calf serum, penicillin (100 U/ml), streptomycin (100 µg/ml) and 2 mM glutamine. HEK 293 cells were transiently transfected with either HERG, HERG/EGFP or EGFP/HERG. The plasmid concentrations were as follows (µg per 35 mm dish containing 1.8 ml of medium): 1.88 µg HERG, 2.27 µg HERG/EGFP, 2.27 µg EGFP/HERG. Transfections were carried out using 7 µl lipofectamine and 200 µl Opti-MEM (Invitrogen, Karlsruhe, Germany). Electrophysiological and fluorescence microscopy studies were performed 48–72 h after transfection.

Electrophysiological Recording

HERG, HERG/EGFP and EGFP/HERG currents were recorded using the whole-cell patch-clamp configuration (Hamill et al. 1981) and an EPC-7 patch-clamp amplifier (Heka Elektronik, Lambrecht, Germany). Patch pipettes were pulled from borosilicate glass capillaries (Hilgenberg, Malsfeld, Germany) and had resistances between 3 and 5 MΩ when filled with pipette solution B. Current signals were filtered at 2 kHz with the help of a Bessel filter (902; Frequency Devices, Haverhill, MA). Stimulation protocols and data acquisition were carried out using a microcomputer equipped with D-A and A-D converters (Digidata 1200 Interface; Axon Instruments, Foster City, CA) and pCLAMP 6.0.2 software (Axon Instruments). The current sample frequency was 50 Hz. At least 50% series resistance compensation was achieved in all experiments. Outward currents flowing from the pipette to the bath solution are indicated by upward deflections. Experiments were performed at room temperature (20–22°C).

The voltage-clamp protocol to study HERG currents was as follows: The holding potential was −80 m*V*, and a voltage step to +10 m*V* was applied for 2 s to evoke HERG currents, followed by a repolarization step to −40 m*V* for 2 s to induce HERG tail currents (stimulation frequency of 0.1 Hz). HERG tail currents were leak-corrected. The activation time course at a test potential of +10 m*V* was described by fitting the rising phase of the activating outward current by a single exponential function. Deactivating tail currents were fitted with two exponential functions and extrapolated to the beginning of the repolarization step in order to calculate the peak tail current amplitude.

The voltage dependence of HERG channel activation was determined from peak tail currents measured at −40 m*V* following 2-s depolarizations to membrane voltages ranging from −40 to +40 m*V* in 10-m*V* steps. Peak tail current amplitudes were normalized to the maximum peak tail current amplitudes. The voltage dependence of channel availability was determined by fitting the values of the normalized tail currents to a Boltzmann equation of the following form:

$$I/I_{\max} = \left\{1 + \exp\left[\left(V_{1/2} - V_{\mathrm{m}}\right)/k\right]\right\}^{-1} \quad (1)$$

where I is the peak tail current amplitude following the test potential V_{m}, $I_{\max}$ is the maximal peak tail current, $V_{½}$ is the potential at which channels are half-maximally activated and k is the slope factor describing channel activation.

The concentration–response relationships for the inhibition of peak tail current amplitudes by domperidone were calculated according to the logistic form of the Hill equation:

$$I/I_{\mathrm{c}} = 1 - \left(1 + 10^{n(px - pK)}\right)^{-1} \quad (2)$$

where I_{c} is the tail current amplitude during the control periods before application of domperidone and I is the tail current amplitude in the presence of domperidone, n is the slope parameter (Hill coefficient), x is the concentration of domperidone and K (= IC_{50}) is the midpoint of the curve with $px = -\log x$ and $pK = -\log IC_{50}$.

Immunocytochemistry

The EGFP-induced fluorescence was used to localize the HERG/EGFP and EGFP/HERG fusion proteins expressed in HEK 293 cells. An anti-HERG antibody was used for the localization of HERG/EGFP and EGFP/HERG channels in the plasma membrane of HEK 293 cells. Transiently transfected HEK 293 cells were grown on sterile polylysine-coated glass coverslips for 24 h. Cells were then washed twice with phosphate-buffered saline (PBS), blocked with 4% bovine serum albumin in PBS for 20 min at 37°C and incubated with primary antibodies at a 1:25 dilution generated against an extracellular epitope located at the linker between the first and second transmembrane domains of the HERG channel for 60 min (37°C). Cells were subsequently rinsed three times in PBS, incubated for 60 min with fluorescently labeled secondary antibodies (TRITC- or FITC-conjugated goat anti-rabbit IgG) at a dilution of 1:200, followed by three washes with PBS. Cells were then fixed with 4% formaldehyde/PBS for 20 min at room temperature. After two final washes with PBS, cells were embedded using mounting medium (Dako Cytomation, Carpinteria, CA).

Imaging was performed with a Zeiss (Thornwood, NY) LSM-510 confocal laser scanning microscope equipped with the META^{TM} system (Zeiss). Cells were illuminated through a water immersion objective lens (C-Apochromat 40x/1.2). Both EGFP fusion proteins (absorption peak at 488 nm) and FITC-labeled antibodies (absorption peak at 495 nm) were excited with an Ar laser at 488 nm, and TRITC-labeled antibodies (absorption peak at 552 nm) were excited with a HeNe laser at 543 nm. The fluorescence intensities of the EGFP fusion proteins (emission peak at 510 nm) and of TRITC-labeled antibodies (emission peak at 570 nm) were distinguished by measuring EGFP-induced fluorescence intensity at 505–550 nm and TRITC-induced fluorescence intensity at 550–700 nm, respectively, using two photomultiplier tubes. The fluorescence intensities of EGFP and FITC-labeled antibodies were distinguished using the META^{TM} system. Multispectral images were obtained at 500–570 nm as a set of two-dimensional images as a function of wavelength. EGFP and FITC have fluorescence spectra that closely overlap with each other (emission peaks 510 and 525 nm, respectively). Best results of color separation were obtained when cells stained with each of the dyes were used to measure a reference spectrum. Spectral overlap between fluorescent dyes could be separated into spectra of each dye by a computational process called "linear unmixing."

For a three-dimensional presentation of cells, optical sections with a diameter of 2 μm were scanned at intervals of 1 μm across the Z axis, and the number of z-scans ranged between 11 and 21. In order to quantify the surface expression of the fusion proteins located at the plasma membrane, two-dimensional images of cells were scanned with optical sections with a diameter of 2 μm across the Z axis through the middle of the cells. The fluorescence intensity values of the secondary antibodies labeled with either FITC or TRITC located at the plasma membrane from cells expressing the fusion constructs were corrected for both background fluorescence and autofluorescence of the cells and related to the cell surface area according to the following equation:

$$F/c = F_{\mathrm{ROI}} \cdot \pi \cdot r^2/2 \cdot \pi \cdot r = F_{\mathrm{ROI}} \cdot r/2 \quad (3)$$

where F is the fluorescence intensity of the labeled secondary antibodies located at the plasma membrane, c is the circumference of a cell (assuming that HEK 293 cells have a spherical form), F_{ROI} is the mean fluorescence intensity of a cell (region of interest, ROI) and r is the radius of a cell. The mean values of the surface fluorescence intensity per circumference of 8–43 cells per transfection were calculated. Intensity values were obtained by calculating the brightness values measured on an arbitrary gray scale from 0 (blackest) to 255 (whitest). In all experiments, confocal microscope settings were maintained constant. The time required for scanning a two-dimensional image was 7.9 s (55 s for a two-dimensional multispectral image obtained at seven wavelength sections between 500 and 570 nm using the META^{TM} system). Laser-scanning confocal microscopy experiments were performed at room temperature (20–22°C).

Solutions and Chemicals

The bath (solution A) contained (in mM) 140 NaCl, 5.6 KCl, 1.2 $MgCl_2$, 2.6 $CaCl_2$ and 10 HEPES, titrated to pH 7.40 with NaOH. The pipette (solution B) contained (in mM) 140 KCl, 5 $MgCl_2$, 10 EGTA, 2 $CaCl_2$, 5 ATP and 5 HEPES, titrated to pH 7.15 with KOH (free $[Ca^{2+}] =$ 50 nM, free $[Mg^{2+}] = 0.7$ mM). Rabbit anti-HERG antibody was obtained from Alomone Labs (Jerusalem, Israel). TRITC- or FITC-conjugated goat anti-rabbit IgG secondary antibodies were obtained from Sigma (St. Louis, MO). Domperidone was purchased from Sigma, and a stock solution of 10 mM domperidone was prepared in dimethyl sulfoxide and applied to solution A to give the final concentrations.

Statistics

The results are expressed as means ± SEM. Equations were fitted using the program Sigma Plot Windows (Jandel Scientific, Tübingen, Germany). Significance was calculated by the two-tailed, nonpaired t-test and $P < 0.05$ was considered significant.

Results

Electrophysiological Properties of HERG/EGFP and EGFP/HERG Channels

At first, the membrane currents in HEK 293 cells transiently expressing HERG channels, HERG/EGFP channels and EGFP/HERG channels were studied (Fig. 1). Depolarizing voltage-clamp steps to membrane potentials ranging from −40 to +40 mV in 10-mV increments from a holding potential of −80 mV elicited time-dependent outward currents in HEK 293 cells expressing HERG, HERG/EGFP and EGFP/HERG channels; after repolarization of the membrane potential to −40 mV, tail currents were observed. Figure 1b shows the current–voltage relationships measured at the end of the initial depolarizing steps in HEK 293 cells transiently transfected with HERG, HERG/EGFP or EGFP/HERG. HERG and EGFP/HERG currents were activated at membrane potentials positive to about −30 mV, and HERG/EGFP currents were activated at membrane potentials positive to about −40 mV. At membrane potentials positive to about 0–10 mV the current-voltage relationships for all three channels showed a marked inward rectification with a negative slope conductance. The current densities at the end of the 2-s depolarizing voltage steps to +20 mV were 31.3 ± 3.5 pA/pF for HERG channels ($n = 38$), 42.2 ± 8.2 pA/pF for HERG/EGFP channels ($n = 18$) and 13.4 ± 1.3 pA/pF for EGFP/HERG channels ($n = 28$). In contrast, in nontransfected HEK 293 cells currents of only small amplitude were observed following the depolarizing voltage pulses (5.0 ± 1.1 pA/pF at a depolarizing test pulse to +20 mV, $n = 7$). Following repolarization to a membrane potential of −40 mV, the tail current densities were 102.1 ± 9.3 pA/pF for HERG channels, 118.8 ± 20.6 pA/pF for HERG/EGFP channels and 29.7 ± 3.6 pA/pF for EGFP/HERG channels. Both current densities at the end of the depolarizing voltage step to +20 mV and tail current densities following repolarization to a membrane potential of −40 mV were significantly smaller for EGFP/HERG channels compared to HERG and HERG/EGFP channels ($P < 0.05$). Figure 1c shows the voltage dependence of steady-state HERG current activation. The values for $V_{½}$ (the potential at which HERG channels were half-maximally activated) and k (the slope factor describing HERG channel activation), respectively, were 0.3 ± 0.4 mV and 8.3 ± 0.3 mV for HERG channels, −14.3 ± 0.4 mV and 7.6 ± 0.3 mV for HERG/EGFP channels and −6.1 ± 0.6 mV and 9.9 ± 0.5 mV for EGFP/HERG channels. The values for $V_{½}$ of the fusion proteins were significantly more negative compared to HERG channels ($P < 0.05$).

The time constants for activation at a depolarizing pulse to +10 mV were significantly ($P < 0.05$) reduced for both HERG channel/EGFP fusion proteins (269 ± 26 ms for HERG/EGFP channels [$n = 47$], 338 ± 29 ms for EGFP/HERG channels [$n = 46$]) compared to HERG channels (1,023 ± 33 ms, $n = 173$). Deactivating tail currents recorded on repolarization to −40 mV from a test potential of +10 mV were fitted by a double exponential function, and the values for the fast deactivation time constants (τ_{fast}) were 144 ± 4 ms for HERG currents, 129 ± 7 ms for

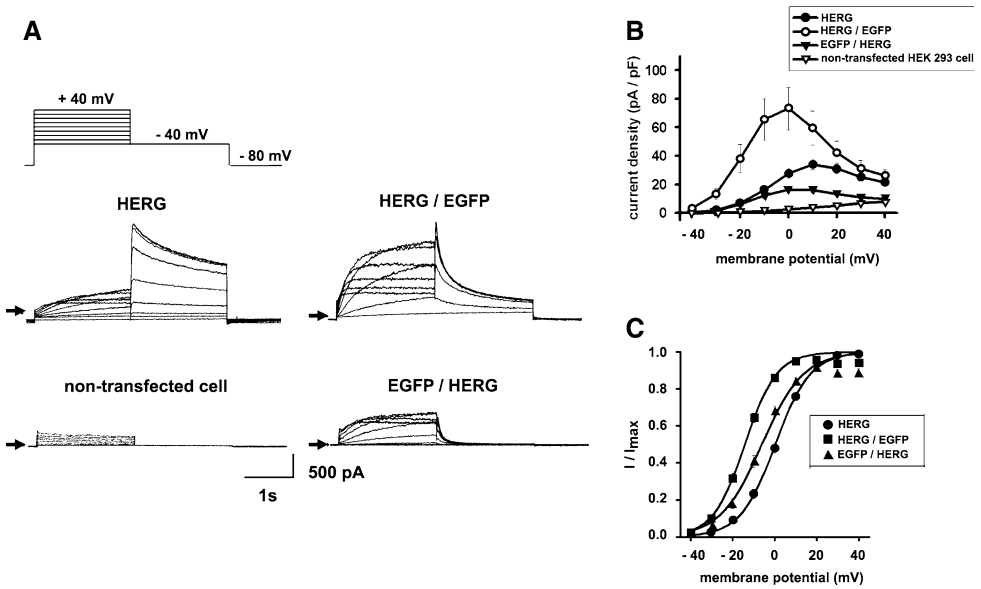

Fig. 1 (**A**) Whole-cell outward currents in HEK 293 cells transiently expressing HERG channels (*middle left traces*), HERG/EGFP channels (*middle right traces*) and EGFP/HERG channels (*lower right traces*) and in a nontransfected HEK 293 cell (*lower left traces*). The voltage-clamp protocol (*upper left trace*) used to study currents was as follows: The holding potential was −80 m*V*, and voltage steps to membrane potentials between −40 and +40 m*V* in increments of 10 m*V* were applied for 2 s to evoke currents, followed by a repolarization step to −40 m*V* for 2 s to induce tail currents. *Arrows* indicate zero current levels. (**B**) Relationships between current density and membrane potential of nontransfected HEK 293 cells (▽) and HEK 293 cells transiently transfected with HERG channels (●), HERG/EGFP channels (◯) and EGFP/HERG channels (▼). The current amplitudes measured at the end of the depolarization steps were normalized to the cell capacitance (ordinate) and plotted against the membrane potentials (abscissa). Symbols represent means and vertical lines the SEM. (**C**) Voltage dependence of steady-state HERG current activation. Peak tail currents (*I*) for HERG channels (●), HERG/EGFP channels (■) and EGFP/HERG channels (▲) at each voltage were normalized to the maximal currents (I_{max}, ordinate) and plotted against the membrane potentials (abscissa). The data were fitted with the Boltzmann function (equation 1) to determine the midpoint of activation ($V_{½}$) and the slope factor (*k*). Symbols represent means and the vertical lines the SEM

HERG/EGFP currents and 83 ± 5 ms for EGFP/HERG currents. The values for the slow deactivation time constants (τ_{slow}) were 1,397 ± 24 ms for HERG currents, 825 ± 36 ms for HERG/EGFP currents and 421 ± 31 ms for EGFP/HERG currents. The fraction of the fast component was calculated as $a_{fast}/(a_{fast} + a_{slow})$, where values for a_{fast} and a_{slow} refer to the amplitudes of the fast and slow components of deactivation. The respective values were 0.1 ± 0.01 for HERG tail currents, 0.3 ± 0.02 for HERG/EGFP tail currents and 0.77 ± 0.02 for EGFP/HERG tail currents. Therefore, for HERG/EGFP tail currents the slow deactivation time constant was significantly ($P < 0.05$) smaller and the fraction of the fast component was significantly larger ($P < 0.05$) compared to HERG channels. For EGFP/HERG channels the deactivating tail currents were markedly reduced compared to both HERG channels and HERG/EGFP channels since both the fast and slow deactivation time constants of the tail currents were markedly smaller and the fraction of the fast component was markedly larger compared to both HERG and HERG/EGFP channels.

Block of HERG/EGFP and EGFP/HERG Currents by Domperidone

In order to study the pharmacological properties of HERG/EGFP and EGFP/HERG channels, the effects of domperidone were tested. Domperidone is a well-known inhibitor of HERG currents (Drolet et al. 2000) and has previously been shown to inhibit HERG currents half-maximally at a concentration of 57 nM (95% confidence interval [CI] 44.4–73.2), and the Hill coefficient was 0.99 (95% CI 0.73–1.25) (Claassen and Zünkler 2005). Under the same experimental conditions, domperidone blocked HERG/EGFP currents half-maximally at a concentration of 62.2 nM (95% CI 54.3–71.7), and the Hill coefficient was 0.99 (95% CI 0.94–1.34). EGFP/HERG currents were blocked by domperidone half-maximally at a concentration of 46.6 nM (95% CI 34.3–63.2), and the Hill coefficient was 0.99 (95% CI 0.67–1.33). There were no significant differences for the IC_{50} values and the Hill coefficients between HERG, HERG/EGFP and EGFP/HERG channels ($P > 0.05$, Fig. 2).

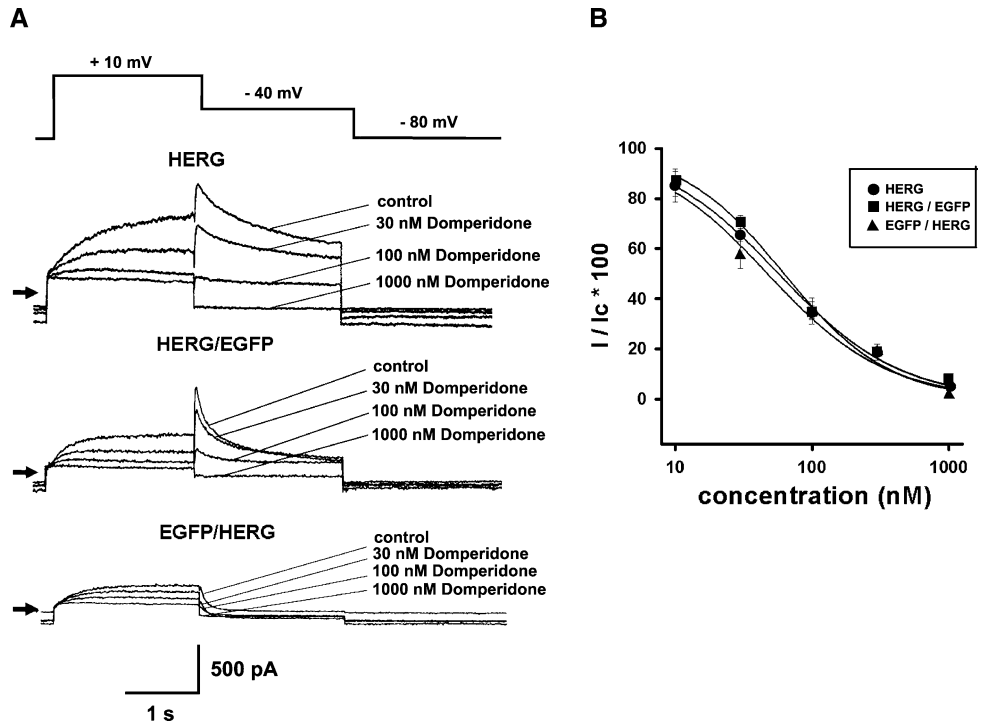

Fig. 2 Effects of domperidone on HERG currents, HERG/EGFP currents and EGFP/HERG currents. (**A**) Current responses at increasing concentrations of domperidone (*lower traces*) to the voltage protocol (*upper trace*). The voltage-clamp protocol used to study HERG, HERG/EGFP and EGFP/HERG currents was as follows: The holding potential was −80 m*V*, and a voltage step to +10 m*V* was applied for 2 s to evoke currents, followed by a repolarization step to −40 m*V* for 2 s to induce tail currents. *Arrows* indicate zero current levels. (**B**) Concentration–response relationships for the inhibition of HERG (●), HERG/EGFP (■) and EGFP/HERG (▲) tail currents by domperidone. Deactivating tail currents were leak-corrected, fitted with two exponential functions and extrapolated to the beginning of the repolarization step in order to calculate the peak tail current amplitude. The ordinate represents current amplitudes in the presence of different concentrations of domperidone (I) in percent of the current amplitudes in the absence of the drug (control, Ic). The abscissa indicates the concentrations of domperidone (logarithmic scale). Symbols represent means and the vertical lines the SEM. Numbers of observations were between 4 and 10 at each concentration tested. The lines are fits to Eq. 2. The concentration–response relationship for the inhibition of HERG currents by domperidone is taken from Claassen and Zünkler (2005)

Plasma Membrane Expression of HERG/EGFP and EGFP/HERG Channels Transiently Expressed in HEK 293 Cells

The cellular distribution and the plasma membrane localization of HERG/EGFP and EGFP/HERG channels transiently expressed in HEK 293 cells were studied. Figure 3 shows three-dimensional images of the fluorescence of HERG/EGFP and EGFP/HERG channels transiently expressed in HEK 293 cells using laser scanning confocal microscopy. The transfection efficiency of both fusion proteins was about 30%. For both fusion proteins an inhomogenous pattern of fluorescence throughout the cytosol and the plasma membrane was observed in all cells studied (six cells from three transfections were evaluated for each fusion protein), whereas the nuclei did not show EGFP-induced fluorescence. To study the localization of HERG/EGFP and EGFP/HERG channels at the plasma membrane, immunocytochemistry with primary anti-HERG antibodies and with fluorescently labeled secondary antibodies was performed. Both fusion proteins were located at the plasma membrane, and an inhomogenous pattern of labeling of both fusion proteins in the plasma membrane was observed (Figs. 3–5). A similar inhomogenous pattern of labeling of wild-type HERG channels stably expressed in HEK 293 cells was observed after immunolabeling with FITC-conjugated primary anti-HERG antibodies (not shown), indicating that both fusion proteins and wild-type HERG channels are located in discrete microdomains in the plasma membrane of HEK 293 cells. The three-dimensional presentations indicated that the extent of labeling with anti-HERG antibodies of HEK 293 cells expressing EGFP/HERG channels was lower compared to cells expressing HERG/EGFP channels. This was further studied by scanning two-dimensional images of cells through the middle of the cells and quantifying the fluorescence intensity values of the secondary labeled antibodies normalized by the circumference of the cells (Fig. 4 with secondary antibodies labeled with TRITC and Fig. 5 with secondary antibodies labeled with FITC). Colocalization of the fusion protein–induced fluorescence and the anti-HERG antibody–induced fluorescence showed that HEK 293 cells expressing HERG/EGFP channels were more

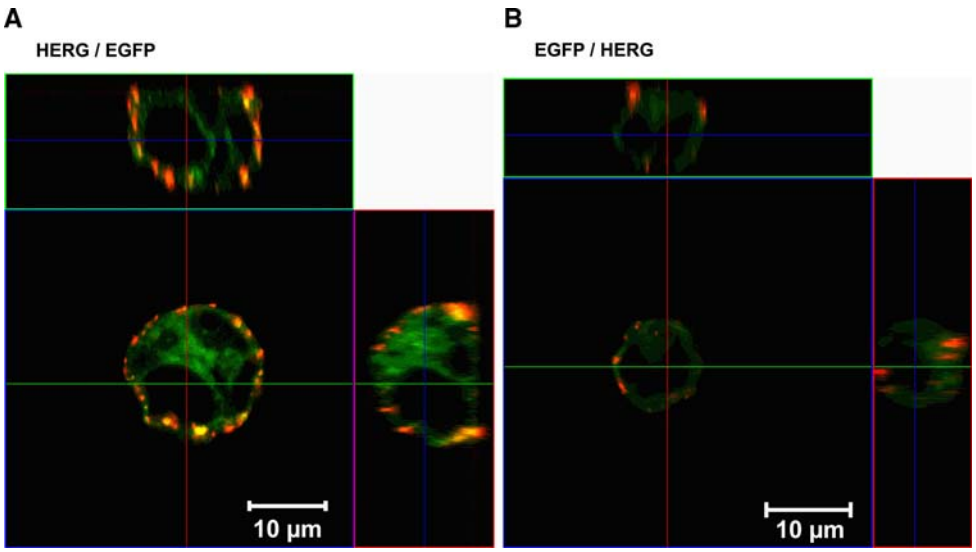

Fig. 3 Three-dimensional images of the subcellular localization of HERG/EGFP channels (**A**) and EGFP/HERG channels (**B**) expressed in HEK 293 cells. Confocal images of cells expressing HERG/EGFP channels (**A**) and EGFP/HERG channels (**B**) (green fluorescence), which were immunolabeled with an anti-HERG channel antibody followed by a TRITC-conjugated secondary antibody (red fluorescence). *Bars* on the right and top of each image represent scans across the Z axis through the cells in the *x* (*top*) and *y* (*right*) directions. Both fusion proteins were located in the cytosol and in the plasma membrane. Nonstained regions within the cells are the nuclei. The orange color after merging of the EGFP- and TRITC-induced fluorescence reveals that both fusion proteins are localized in the plasma membrane. Note the inhomogenous pattern of labeling of both fusion proteins with the primary anti-HERG antibodies and fluorescently labeled secondary antibodies in the plasma membrane and the lower extent of labeling with anti-HERG antibodies of HEK 293 cells expressing EGFP/HERG channels compared to HEK 293 cells expressing HERG/EGFP channels

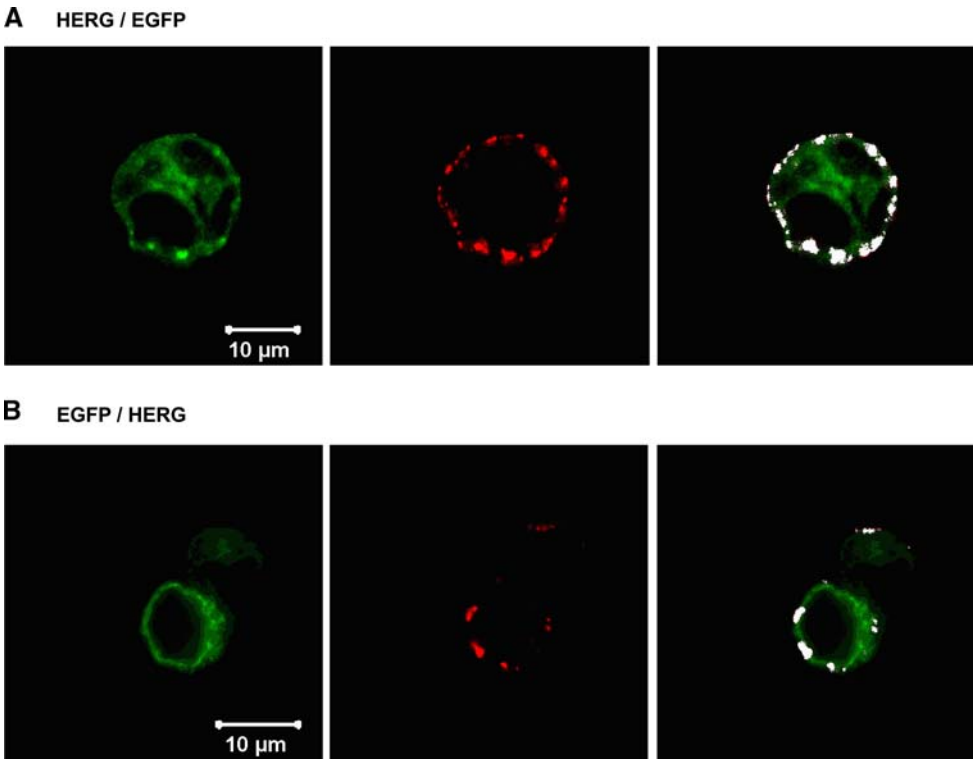

Fig. 4 Confocal images of HEK 293 cells expressing HERG/EGFP channels (**A**) and EGFP/HERG channels (**B**) (green fluorescence, *left*) which were immunolabeled with an anti-HERG channel antibody followed by a TRITC-conjugated secondary antibody (red fluorescence, *middle*). The white color after merging of the EGFP- and TRITC-induced fluorescence (*right*) reveals that both fusion proteins are localized in the plasma membrane. Note that the areas of colocalization in the plasma membrane are inhomogenous and the extent of labeling with anti-HERG antibodies of HEK 293 cells expressing EGFP/HERG channels is lower compared to HEK 293 cells expressing HERG/EGFP channels

intensively stained by antibodies than HEK 293 cells expressing EGFP/HERG channels. Quantification of fluorescence signals of TRITC-conjugated secondary antibodies resulted in fluorescence intensity values related to the cell circumference (F/c) of 9.7 ± 1.6 for HERG/EGFP channel expressing-cells ($n = 3$ transfections) and 4.0 ± 0.8 for

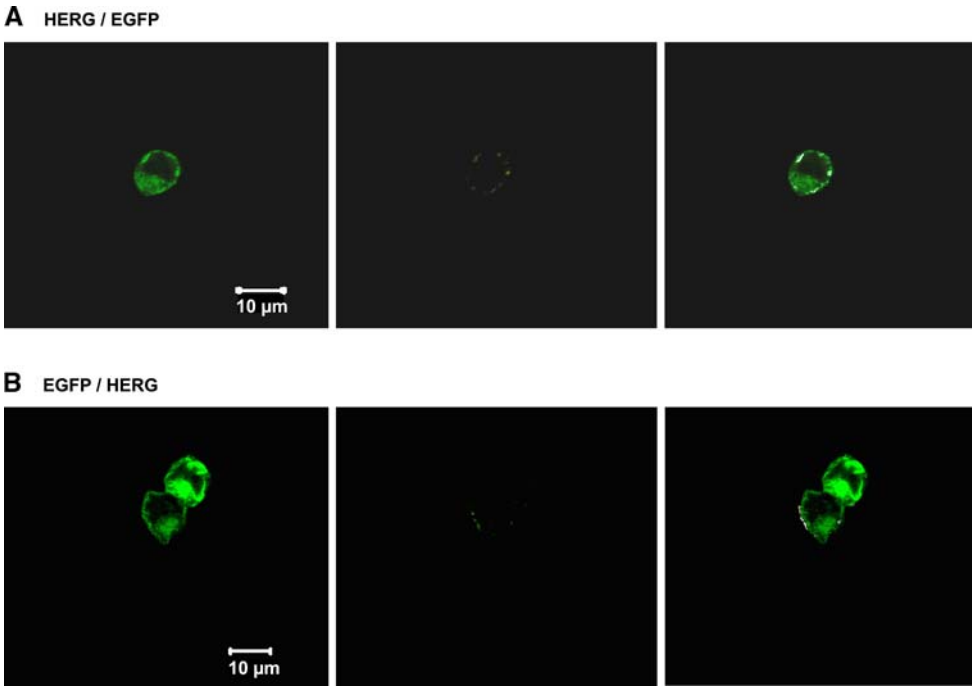

Fig. 5 Confocal images of HEK 293 cells expressing HERG/EGFP channels (**A**) and EGFP/HERG channels (**B**) (green fluorescence, *left*) which were immunolabeled with an anti-HERG channel antibody followed by a FITC-conjugated secondary antibody (green fluorescence, *middle*) generated with the META^{TM} system of the laser scanning microscope. The white color after merging of the EGFP- and FITC-induced fluorescence (*right*) reveals that both fusion proteins are localized in the plasma membrane. Note that the areas of colocalization in the plasma membrane are inhomogenous and the extent of labeling with anti-HERG antibodies of HEK 293 cells expressing EGFP/HERG channels is lower compared to HEK 293 cells expressing HERG/EGFP channels

EGFP/HERG channel–expressing cells ($n = 5$), and the difference of these values was statistically significant ($P < 0.05$). Similar results were obtained by quantification of fluorescence signals of FITC-conjugated secondary antibodies obtained with the help of the META^{TM} system with values of 8.5 ± 1.8 for HERG/EGFP channel–expressing cells ($n = 4$) and 3.4 ± 0.7 for EGFP/HERG channel–expressing cells ($n = 4$), and the difference of these values was again statistically significant ($P < 0.05$). These differences suggest a reduced plasma membrane expression of EGFP/HERG channels compared to HERG/EGFP channels.

Discussion

The present study compares the electrophysiological and pharmacological properties and the cellular localization of HERG channels tagged with EGFP either to the C or N terminus expressed in HEK 293 cells. Trafficking defects in LQT2 are commonly studied using EGFP tagged to mutated HERG channels.

About 200 LQT2-associated HERG mutations have been described. Mutations in the N-terminal domain are associated with altered deactivation. Deletion of the first 354–370 amino acids of the HERG channel results in a channel with substantially faster deactivation, and point mutations in the N-terminal domain and smaller deletions also lead to accelerated deactivation. The N terminus of the HERG channel shows similarity to the Per-Arnt-Sim (PAS) domains, and the N-terminal PAS domain may interact with the S4–S5 linker, thereby controlling channel deactivation (review in Vandenberg et al. 2004). The observation that the deactivation kinetics of EGFP/HERG channels was fast may indicate that EGFP fused to the N-terminal domain of the HERG channel prevents the interaction of the N-terminal PAS domain with the S4–S5 linker.

The biophysical properties of HERG/EGFP channels as determined in the present study were similar to those of HERG channels. This is consistent with previous finding that HERG channels with a GFP molecule tagged to the carboxyl terminus had electrophysiological characteristics similar to the channel encoded by native HERG, which indicated that GFP tagged to the carboxyl terminus affects neither HERG/GFP targeting to the cell surface nor its function (Petrecca et al. 1999).

For EGFP/HERG channels, the peak tail current density was reduced compared to both wild-type HERG channels and HERG/EGFP channels. HEK 293 cells expressing EGFP/HERG channels were less intensively marked by anti-HERG antibodies than HEK 293 cells expressing

HERG/EGFP channels. These observations suggest reduced plasma membrane expression of EGFP/HERG channels compared to HERG/EGFP channels. Similarly, mutations in the PAS domain of the N-terminal domain of the HERG channel result in defective trafficking of the protein to the cell membrane (Paulussen et al. 2002). Mutations in the C-terminal domain are associated with a range of defects including effects on subunit assembly (review in Vandenberg et al. 2004), and mutations located in the C-terminal domain of the HERG channel associated with LQT2 failed to form functional channels due to ineffective trafficking to the plasma membrane (Teng et al. 2004; Sasano et al. 2004; Paulussen et al. 2005). The C-terminal region of the HERG channel contains an endoplasmic reticulum (ER) retention signal, and a key function of the C-terminal 104 amino acids is to mask the arg-gly-arg ER retention signal in properly folded channels. This ER retention signal becomes exposed when the C terminus is truncated (Kupershmidt et al. 2002). This function of the C-terminal region of the HERG channel does not seem to be altered by fusing EGFP to the C terminus of the HERG channel since the expression of HERG/EGFP channels was not reduced. Studies performed with glutamate receptor 3/GFP fusion proteins showed divergent results since the fusion of GFP to the amino terminus did not alter the properties, whereas tagging GFP to the carboxyl terminus led to receptors that produced larger currents in response to agonist application that were correlated with increases in both fluorescence and amount of protein in the plasma membrane (Limon et al. 2007).

Most drugs block HERG channels primarily in the open and/or inactivated state, and the binding site of most HERG channel blockers is located in the central cavity of the channel between the selectivity filter and the activation gate (review in Sanguinetti and Mitcheson 2005). It is suggested that the binding site for domperidone is also located in the central cavity of the channel since block of HERG currents by domperidone was stronger at more positive membrane potentials, which indicates that domperidone has a predominant affinity for the open and/or inactivated states of the HERG channel (Claassen and Zünkler 2005). Therefore, it seems not surprising that fusion of EGFP either to the N or C terminus of the HERG channel does not influence the domperidone sensitivity of the fusion proteins since both the N- and C-terminal cytoplasmic domains are located some distance from the central cavity of the HERG channel. This is in line with the previous finding that the HERG/GFP-induced delayed rectifier current was completely blocked by 1 μM E−4031, a selective inhibitor of I_{Kr} (Petrecca et al. 1999).

For both fusion proteins an inhomogenous pattern of fluorescence throughout the cytosol was observed. Fusion proteins consisting of HERG and either EGFP or GFP fused to its N terminus have been observed intracellularly in the ER, the perinuclear space and the plasma membrane, whereas the nucleus was not stained (Furutani et al. 1999; Jenke et al. 2003). Similarly, a fusion protein consisting of HERG and GFP fused to its C terminus has been observed in both the ER and the plasma membrane (Rossenbacker et al. 2005).

Immunocytochemistry studies performed with primary anti-HERG antibodies and with fluorescently labeled secondary antibodies showed an inhomogenous pattern of labeling of both fusion proteins in the plasma membrane, demonstrating that both EGFP/HERG channels and HERG/EHGFP channels are located in discrete microdomains of the plasma membrane of HEK 293 cells expressing the fusion proteins. The plasma membrane is not a simple fluid bilayer; in fact, there are microdomains within the plasma membrane known as "lipid rafts." Lipid rafts are comprised of tightly packed glycosphingolipids, sphingomyelin and cholesterol. Lipid rafts localize membrane proteins like ion channels to specific cell-surface regions. Additionally, protein–protein interactions between ion channels and scaffolding proteins (such as PSD-95) and the cytoskeleton represent important mechanisms for localizing ion channels with the modulatory pathways that regulate them (review in O′Connell, Martens and Tamkun 2004). Cardiac channel subunits known to localize in lipid rafts include Kv1.4, Kv1.5, Kv2.1, Kv4, Kir2, Kir3, K_{ATP}, Nav and Cav. However, there is still limited knowledge about the lipid raft localization of HERG channels (review in Maguy, Hebert and Nattel 2006). HEK 293 cells are a meaningful model system which helps to explore the mechanisms underlying trafficking and cell surface localization as demonstrated previously for Kv2.1 (O′Connell and Tamkun 2005). The observation of the present study that both fusion proteins are located in discrete microdomains of the plasma membrane of HEK 293 cells was confirmed in preliminary experiments for HERG channels stably expressed in HEK 293 cells and immunolabeled with FITC-conjugated primary anti-HERG antibodies (not shown). These observations might point toward a lipid raft localization of HERG channels in HEK 293 cells.

In conclusion, K^+ currents with tail currents characteristic for HERG channels were observed for both EGFP/HERG channels and HERG/EGFP channels expressed in HEK 293 cells. The sensitivity to domperidone was similar between wild-type HERG, EGFP/HERG and HERG/EGFP channels. Both fusion proteins were localized in the cytoplasm and on discrete microdomains in the plasma membrane. For EGFP/HERG channels, the deactivation kinetics was faster and the peak tail current density reduced compared to both wild-type HERG channels and HERG/EGFP channels. The extent of labeling with anti-HERG antibodies of HEK 293 cells expressing EGFP/HERG channels was less compared to HEK 293 cells expressing

HERG/EGFP channels, which suggests that EGFP/HERG channels themselves might have a protein trafficking defect. However, the properties of HERG/EGFP channels seem to be similar to those of wild-type HERG channels. These observations support the conclusion (Limon et al. 2007) that extensive functional characterization of the tagged receptor is recommended for proper interpretation of results obtained with tagged receptors. The observation that EGFP tagged to the C terminus of the HERG channel does not markedly alter the properties of HERG channels indicates that this construct might be especially useful for the study of receptor–ligand interactions, e.g., by using two-color fluorescence cross-correlation spectroscopy.

Acknowledgement We thank Dr. A. I. Roth for critically reading the manuscript and Ms. A. Wessel for preparing the figures.

References

Anderson CL, Delisle BP, Anson BD, Kilby JA, Will ML, Tester DJ, Gong Q, Zhou Z, Ackerman MJ, January CT (2006) Most LQT2 mutations reduce Kv11.1 (hERG) current by a class 2 (trafficking-deficient) mechanism. Circulation 113:365–373

Claassen S, Zünkler BJ (2005) Comparison of the effects of metoclopramide and domperidone on HERG channels. Pharmacology 74:31–36

Cordes JS, Sun Z, Lloyd DB, Bradley JA, Opsahl AC, Tengowski MW, Chen X, Zhou J (2005) Pentamidine reduces hERG expression to prolong the QT interval. Br J Pharmacol 145: 15–23

Curran ME, Splawski I, Timothy KW, Vincent GM, Green ED, Keating MT (1995) A molecular basis for cardiac arrhythmia: HERG mutations cause long QT syndrome. Cell 80:795–803

Drolet B, Rousseau G, Daleau P, Cardinal R, Turgeon J (2000) Domperidone should not be considered a no-risk alternative to cisapride in the treatment of gastrointestinal motility disorders. Circulation 102:1883–1885

Ficker E, Kuryshev YA, Dennis AT, Obejero-Paz C, Wang L, Hawryluk P, Wible BA, Brown AM (2004) Mechanisms of arsenic-induced prolongation of cardiac repolarization. Mol Pharmacol 66:33–44

Furutani M, Trudeau MC, Hagiwara N, Seki A, Gong Q, Zhou Z, Imamura S, Nagashima H, Kasanuki H, Takao A, Momma K, January CT, Robertson GA, Matsuoka R (1999) Novel mechanism associated with an inherited cardiac arrhythmia: defective protein trafficking by the mutant HERG (G601S) potassium channel. Circulation 99:2290–2294

Hamill OP, Marty A, Neher E, Sakmann B, Sigworth FJ (1981) Improved patch-clamp techniques for high-resolution current recordings from cells and cell-free membrane patches. Pfluegers Arch 391:85–100

Ho SN, Hunt HD, Horton RM, Pullen JK, Pease LR (1989) Site-directed mutagenesis by overlap extension using the polymerase chain reaction. Gene 77:51–59

Jenke M, Sanchez A, Monje F, Stühmer W, Weseloh RM, Pardo LA (2003) C-terminal domains implicated in the functional surface expression of potassium channels. EMBO J 22:395–403

Kupershmidt S, Yang T, Chanthaphaychith S, Wang Z, Towbin JA, Roden DM (2002) Defective human ether-a-go-go-related gene trafficking linked to an endoplasmic retention signal in the C-terminus. J Biol Chem 277:27442–27448

Kuryshev YA, Ficker E, Wang L, Hawryluk P, Dennis AT, Wible BA, Brown AM, Kang J, Chen X-L, Sawamura K, Reynolds W, Rampe D (2005) Pentamidine-induced long QT syndrome and block of hERG trafficking. J Pharmacol Exp Ther 312: 316–323

Limon A, Reyes-Ruiz JM, Eusebi F, Miledi R (2007) Properties of GluR3 receptors tagged with GFP at the amino or carboxyl terminus. Proc Natl Acad Sci USA 104:15526–15530

Maguy A, Hebert TE, Nattel S (2006) Involvement of lipid rafts and caveolae in cardiac ion channel function. Cardiovasc Res 69:798–807

O′Connell KMS, Tamkun MM (2005) Targeting of voltage-gated potassium channel isoforms to distinct cell surface microdomains. J Cell Sci 118:2155–2166

O′Connell KMS, Martens JR, Tamkun MM (2004) Localization of ion channels to lipid raft domains within the cardiovascular system. Trends Cardiovasc Med 14:37–42

Paulussen A, Raes A, Matthijs G, Snyders DJ, Cohen N, Aerssens J (2002) A novel mutation (T65P) in the PAS domain of the human potassium channel HERG results in the long QT syndrome by trafficking deficiency. J Biol Chem 277:48610–48616

Paulussen ADC, Raes A, Jongbloed RJ, Gilissen RAHJ, Wilde AAM, Snyders DJ, Smeets HJM, Aerssens J (2005) HERG mutation predicts short QT based on channel kinetics but causes long QT by heterotetrameric trafficking deficiency. Cardiovasc Res 67:467–475

Petrecca K, Atanasiu R, Akhavan A, Shrier A (1999) *N*-Linked glycosylation sites determine HERG channel surface membrane expression. J Physiol 515:41–48

Rossenbacker T, Mubagwa K, Jongbloed RJ, Vereecke J, Devriendt K, Gewillig M, Carmeliet E, Collen D, Heidbüchel H, Carmeliet P (2005) Novel mutation in the Per-Arnt-Sim domain of KCNH2 causes a malignant form of long-QT syndrome. Circulation 111:961–968

Sanguinetti MC, Mitcheson JS (2005) Predicting drug–hERG channel interactions that cause acquired long QT syndrome. Trends Pharmacol Sci 26:119–124

Sanguinetti MC, Jiang C, Curran ME, Keating MT (1995) A mechanistic link between an inherited and an acquired cardiac arrhythmia. Cell 81:299–307

Sasano T, Ueda K, Orikabe M, Hirano Y, Kawano S, Yasunami M, Isobe M, Kimura A, Hiraoka M (2004) Novel C-terminus frameshift mutation, 1122fs/147, of HERG in LQT2: additional amino acids generated by frameshift cause accelerated inactivation. J Mol Cell Cardiol 37:1205–1211

Splawski I, Shen J, Timothy KW, Lehmann MH, Priori S, Robinson JL, Moss AJ, Schwartz PJ, Towbin JA, Vincent GM, Keating MT (2000) Spectrum of mutations in long-QT syndrome genes: KVLQT1, HERG, SCN5A, KCNE1, and KCNE2. Circulation 102:1178–1185

Sun H, Liu X, Xiong Q, Shikano S, Li M (2006) Chronic inhibition of cardiac Kir2.1 and hERG potassium channels by celastrol with dual effects on both ion conductivity and protein trafficking. J Biol Chem 281:5877–5884

Teng S, Ma L, Dong Y, Lin C, Ye J, Bähring R, Vardanyan V, Yang Y, Lin Z, Pongs O, Hui R (2004) Clinical and electrophysiological characterization of a novel mutation R863X in HERG C-terminus associated with long QT syndrome. J Mol Med 82:189–196

Trudeau MC, Warmke JW, Ganetzky B, Robertson GA (1995) HERG, a human inward rectifier in the voltage-gated potassium channel family. Science 269:92–95

Vandenberg JI, Torres AM, Campbell TJ, Kuchel PW (2004) The HERG K^+ channel: progress in understanding the molecular basis of its unusual gating kinetics. Eur Biophys J 33:89–97

Wang L, Wible BA, Wan X, Ficker E (2007) Cardiac glycosides as novel inhibitors of human ether-a-go-go-related gene channel trafficking. J Pharmacol Exp Ther 320:525–534

Warmke JW, Ganetzky B (1994) A family of potassium channel genes related to eag in *Drosophila* and mammals. Proc Natl Acad Sci USA 91:3438–3442

Zünkler BJ (2006) Human ether-a-go-go-related (HERG) gene and ATP-sensitive potassium channels as targets for adverse drug effects. Pharmacol Ther 112:12–37